Nuclear Quadrupole Relaxation and Chemical Shift of Xe^{131} in Liquid and Solid Xenon*†

WILLIAM W. WARREN, JR.,‡ AND R. E. NORBERG
Department of Physics, Washington University, St. Louis, Missouri
(Received 24 January 1966)

The spin-lattice relaxation time and temperature-dependent chemical shift of Xe^{131} in liquid and solid xenon have been measured between 9 and 250°K. A calculation of the transition probabilities for quadrupolar relaxation of Xe^{131} in solid xenon via the Raman process is described. The calculation is based on the theory of Van Kranendonk, modified for the case of a face-centered cubic lattice with electric-field gradients arising from exchange and van der Waals interactions. The data are shown to verify the predicted temperature dependence of T_1 in the solid above 9°K and the absolute magnitude of T_1 at 100°K. It is demonstrated that the temperature dependence of the data is consistent with the temperature variation of the Debye temperature Θ obtained by Packard and Swenson from specific-heat measurements. Quadrupolar relaxation via diffusing impurities was observed at temperatures near the melting point in solid xenon samples containing roughly 1% air. The quadrupolar relaxation time of Xe^{131} in liquid xenon was found to vary exponentially with temperature with an "activation energy" $E_A=640\pm30$ cal/mole. This "activation energy" is approximately one-half as large as values previously obtained for the activation energy of self-diffusion in liquid xenon. Measurements of the chemical shift of Xe^{131} indicate that the local field increases linearly with density in liquid and solid xenon. Least-squares fits to the data yield the change ΔH of the external resonant field with density: $-(1/H_0)[\partial(\Delta H)/\partial\rho]=(5.1\pm0.5)\times10^{-7}$ (amagat)$^{-1}$ in liquid xenon and $-(1/H_0)[\partial(\Delta H)/\partial\rho]=(18.2\pm1.1)\times10^{-7}$ (amagat)$^{-1}$ in solid xenon. These data support the previous Xe^{129} shift data of Yen and Norberg but disagree with more recent measurements by Brinkmann and Carr of the density dependence of the Xe^{129} shift in solid xenon.

I. INTRODUCTION

INVESTIGATION of nuclear quadrupole relaxation and chemical shifts is a useful means of studying electronic structure and bonding in nonmetallic liquids and solids. Although quadrupole relaxation and chemical shifts have been observed in a number of ionic and covalent solids, there have been no experiments involving quadrupolar nuclei in the condensed phases of the rare gases. The comparative ease with which the interactions (exchange and Van der Waals) between rare-gas atoms may be treated theoretically makes these systems attractive for comparison of experiment and theory. Experiments involving quadrupole relaxation and chemical shifts in liquid and solid rare gases are thus of interest as a means of (1) testing the general theories of these phenomena in a particularly simple type of system and (2) obtaining new information about electronic structure, internal electric-field gradients and thermal atomic motion in liquid and solid rare gases.

Xe^{131} (spin $\frac{3}{2}$) is the most abundant (21.24%) magnetic rare-gas isotope having a nuclear quadrupole moment. The other magnetic isotope of xenon is Xe^{129} (spin $\frac{1}{2}$) with a natural abundance of 26.24%. This species has been the subject of a number of previous nuclear-magnetic-resonance investigations of xenon.[1–4] The present paper describes the results of pulsed-nuclear-magnetic-resonance measurements of the spin-lattice relaxation time and temperature-dependent chemical shift of Xe^{131} in liquid and solid xenon.[5] In addition, the theory of nuclear quadrupole relaxation in a rare-gas solid is discussed and the probabilities are computed for transitions induced by the two-phonon Raman process for Xe^{131} in solid xenon.

II. APPARATUS AND MEASUREMENT TECHNIQUES

Relaxation-time and chemical-shift measurements were made with a coherent pulsed NMR spectrometer operating at 3.0 Mc/sec. Coherent radio-frequency pulse sequences were obtained with a Blume rf gate[6] whose output was amplified by three stages of class C rf amplification and applied to the single transmitter-receiver coil. Nuclear free precession signals from the coil were amplified by a high-gain, low-noise receiver and mixed with a constant 3.0-Mc/sec reference signal for coherent or phase-sensitive detection. The reference signal originated in the master rf oscillator and was phase-shifted with a General Radio 314-S86 variable delay line so as to be in phase with the nuclear signal. The combined reference and nuclear signals were demodulated by a diode detector and displayed through a

* Based on a thesis submitted by William W. Warren, Jr., in partial fulfillment of the requirements for the degree of Doctor of Philosophy in the Graduate School of Arts and Sciences, Washington University.

† Supported by U. S. Army Grant DA-ARO-D-31-124-G564 and an equipment loan contract from the Office of Naval Research.

‡ National Science Foundation Cooperative Graduate Fellow, 1962–65. Present address: Department of Physics, University of California, Los Angeles, California.

[1] R. L. Streever and H. Y. Carr, Phys. Rev. **121**, 20 (1961).
[2] E. R. Hunt and H. Y. Carr, Phys. Rev. **130**, 2302 (1963).
[3] W. M. Yen and R. E. Norberg, Phys. Rev. **131**, 269 (1963).
[4] D. Brinkmann, Phys. Rev. Letters **13**, 187 (1964).
[5] The portion of this work dealing with chemical shifts has been described in preliminary form: W. W. Warren, Bull. Am. Phys. Soc. **9**, 733 (1964).
[6] R. J. Blume, Rev. Sci. Instr. **32**, 554 (1961).

boxcar integrator.[7] The integrator supplied the integrated signal amplitude to a graphic recorder and simultaneously permitted the signal to be observed on an oscilloscope for photographic recording.

Spin-lattice relaxation times shorter than 5 sec were measured with 180°–90° pulse sequences. The amplitude of the free-induction decay following the 90° pulse was observed as a function of the spacing τ between the 180° and 90° pulses. This interval was established by a Tektronix 162 waveform generator and was known to within $\pm 2\%$. The data were analyzed by fitting

$$\ln[1-s(\tau)/s(\infty)] \quad \text{versus} \quad \tau$$

to a straight line by the method of least squares. The slope then yielded the spin-lattice relaxation time T_1. For most measurements, the standard error of the slope was less than 10%. Within the experimental scatter, single exponential behavior was observed in all cases.

At temperatures for which T_1 was greater than 200 msec, data were recorded photographically. The oscilloscope was triggered by the 90° timing pulse and the free induction decay was photographed for six or seven different pulse spacings. The equilibrium signal was observed with a single 90° pulse. In every case, a time of at least $5T_1$ was permitted to elapse between sequences. Some integration of the data was achieved by repeating a given 180°–90° sequence several times and obtaining a multipole exposure.

Values of T_1 less than 200 msec could be measured with the boxcar integrator and much greater accuracy achieved. The procedure for measuring T_1 with the boxcar was the same as the photographic technique except that signal heights for the various 180°–90° intervals were integrated and then recorded with the graphic recorder.

Relaxation times longer than 5 sec were measured by the "saturation-90°" technique. After the nuclear spin system had been saturated by a rapid sequence of 90° pulses, the recovery of the magnetization was observed with a 90° pulse. Because of the difficulty of maintaining exact resonance when T_1 was long, free induction decays were detected by ordinary diode detection (no reference signal) and recorded photographically. The need to obtain the value of the equilibrium magnetization for analysis of the data was obviated by the use of the delayed function plot[8]:

$$S(t+\Delta) \quad \text{versus} \quad S(t), \quad \Delta < T_1.$$

The value of T_1 was obtained from the slope of the data by the least-squares method.

Temperature-dependent shifts of the Xe^{131} resonance were observed relative to a proton resonance obtained with a transistorized crystal-controlled marginal oscillator.[9] The oscillator operated at a nominal frequency of 36.6 Mc/sec enabling both the Xe^{131} and H^1 resonances to be obtained in approximately the same magnetic field. The proton probe was equipped with Helmholtz coils for 60-cps field modulation and static field bias. The latter was achieved by superimposing a dc current on the 60-cps modulation current to slightly bias the magnetic field at the site of the proton resonance and permit both resonances to be observed in the same external field. When the magnetic field was adjusted to exact Xe^{131} resonance at a given temperature by zero beating with the 3.0 Mc/sec reference signal, the shifts appeared as changes in the dc bias current required to achieve exact proton resonance. Since the shifts were small compared to the total applied field, the required changes of field at the proton site were the same as the shifts of the xenon resonance.

The magnetic field produced by the bias coils at the position of the proton sample was calibrated in terms of the measured voltage drop across a series 1-Ω resistor. The calibration measurements were carried out with the modulation-bias coils in the magnet gap at the same position as when measuring resonance shifts. The calibration therefore included the enhancing effects of the pole pieces on the bias field. The estimated error in the calibration was $\pm 6\%$. The bias coils were sufficiently far removed from the xenon sample that the bias field at the xenon sample was negligible.

Shift measurements were made relative to the resonant field value at an arbitrary temperature of 130°K. In the course of each run, the bias field at this temperature was measured periodically to check for drifts. Since the method automatically accounted for magnet drifts, the only instabilities affecting the data were changes in the master oscillator and marginal oscillator frequencies. The reproducibility of the data indicated that these changes were less than the usual reading error. The latter, which arose from the widths of the Xe^{131} and H^1 resonances, was estimated to be ± 0.05 G.

Sample temperatures between 4.2 and 250°K were obtained in a double glass liquid-helium Dewar vessel. Samples were obtained by condensing xenon gas into a cylindrical nylon sample chamber which was 1.00 in. long by 0.450-in. diameter. Temperatures higher than the bath temperatures were obtained with a resistive heater wound on a copper can surrounding the sample container. Studies of liquid xenon at temperatures up to 250°K were made by applying up to 30-atm pressure with helium gas. Temperatures were measured with either copper versus constantan or gold-cobalt versus normal silver thermocouples located in the wall of the nylon chamber. The chamber and heater were enclosed in a brass can containing helium gas for thermal contact with the liquid-nitrogen or liquid-helium bath.

[7] J. Reichert and J. Townsend, Rev. Sci. Instr. **35**, 1692 (1964).
[8] P. C. Mangelsdorf, J. Appl. Phys. **30**, 442 (1959).
[9] R. L. Garwin, A. M. Patlach, and H. A. Reich, Rev. Sci. Instr. **30**, 79 (1959).

Normally, temperatures could be maintained to within ± 1°K during a T_1 or shift measurement.

The xenon gas used for these experiments was supplied by Linde[10] with a specified impurity content of less than 5 ppm of O_2 and less than 85 ppm of Kr, N_2, H_2, H_2O, and hydrocarbons combined. For some experiments, the sample was doped with air in an approximate concentration of a few parts per thousand. "Clean" sample experiments were run as follows. All xenon was removed from the system and the sample handling system was pumped down for several days while metal parts of the system were outgassed. After cleaning, the sample storage cylinder was refilled with fresh Linde xenon. Throughout the course of the "clean" sample experiments, the xenon gas pressure was maintained at several atmospheres so that the sample could not be contaminated by leaks into the sample system. No runs under helium pressure were made with the "clean" sample.

III. SPIN-LATTICE RELAXATION

In systems of nuclei with spins greater than $\frac{1}{2}$, the dominant spin-lattice coupling is often provided by the interaction of the nuclear quadrupole moment with time-dependent electric-field gradients. In the present experiments, the spin-lattice relaxation times of Xe^{131} were orders of magnitude shorter than those of Xe^{129} in spite of the larger magnetic moment and greater abundance of Xe^{129}. This strongly suggests that quadrupole interactions of the Xe^{131} nuclei are responsible for relaxation of this isotope in liquid and solid xenon.

A. Theory

The quadrupole Hamiltonian for a single nucleus with spin I and quadrupole moment Q may be written[11]

$$\mathcal{H}_Q=\sum_\mu Q_\mu V_{-\mu}, \tag{1}$$

where

$$\begin{aligned} &Q_0=A(3I_z^2-I^2), && V_0=V_{zz},\\ &Q_{\pm 1}=A(I_\pm I_z+I_zI_\pm), && V_{\pm 1}=V_{xz}\pm iV_{yz},\\ &Q_{\pm 2}=AI_\pm^2, && V_{\pm 2}=\tfrac{1}{2}(V_{xx}-V_{yy})\pm iV_{xy}, \end{aligned} \tag{2}$$

in which $A=eQ/4I(2I-1)$, $I_\pm=I_x\pm iI_y$ and V is the electric potential at the site of the nucleus. In these experiments,

$$\langle\mathcal{H}_Q\rangle\ll\langle\mathcal{H}_{\text{Zeeman}}\rangle.$$

The Hamiltonian (1) has matrix elements between nuclear Zeeman levels differing by $\Delta m=\pm 1$, ± 2. Electric-field gradients which are time-dependent with a spectrum containing frequencies near the Larmor frequency ω_0 or near $2\omega_0$ can induce transitions between Zeeman states and produce relaxation.

If the effects of spin-spin (dipolar) interactions are ignored, it can be shown that after the application of a 180° pulse, the magnetization M_z of a system of nuclei with $I=\frac{3}{2}$ will recover to equilibrium with a time dependence of the form

$$1-M_z(t)/M_z(\infty)=Ae^{-2W_2t}+Be^{-2W_1t}, \tag{3}$$

where W_1 and W_2 are the probabilities for transitions between Zeeman states differing by $\Delta m=\pm 1$, ± 2, respectively,

$$\begin{aligned} &W_1\equiv W_{3/2,1/2}=W_{-1/2,-3/2},\\ &W_2\equiv W_{3/2,-1/2}=W_{1/2,-3/2}. \end{aligned} \tag{4}$$

In a situation where spin-spin interactions are sufficiently strong, one may assume that after a time of the order of the spin-spin relaxation time T_2 following an initial rf pulse, the system can be described by a spin temperature different from the lattice temperature. Under these conditions it has been shown[12] that the system will relax exponentially to the temperature of the lattice with a single time constant. For $I=\frac{3}{2}$, the relaxation time is given by

$$1/T_1=\tfrac{2}{5}(W_1+4W_2). \tag{5}$$

The theory of spin-lattice relaxation thus reduces to the calculation of the transition probabilities W_1 and W_2. In what follows, the transition probabilities will be calculated for a solid xenon crystal in which the time-dependent electric-field gradients are produced by the thermal vibrations of the crystal lattice.

1. Theory of Quadrupole Relaxation via Thermal Phonons in Rare-Gas Solids

The importance of nuclear quadrupole relaxation in solids was first recognized by Pound,[13] who observed that relaxation times of the correct order of magnitude could be calculated for certain quadrupolar nuclei if one replaced the dipolar interaction by the quadrupolar interaction in the Waller theory of dipolar relaxation.[14] The Waller theory predicts transition probabilities arising from modulation of the dipolar interaction by vibrations of the crystal lattice (phonons). Although these calculated dipolar transition probabilities are much too small, the greater strength of the quadrupole interaction leads to predictions in much better agreement with experiment. It has been generally accepted, therefore, that the quadrupole-phonon interaction is responsible for spin-lattice relaxation of many nuclei with spin greater than $\frac{1}{2}$ in nonmetallic solids. Quadrupole-phonon relaxation has been observed previously

[10] Union Carbide Corporation, Linde Division, Rare Gas Department, 270 Park Avenue, New York, New York, 10017.

[11] M. H. Cohen and F. Reif, in *Solid State Physics*, edited by F. Seitz and D. Turnbull (Academic Press Inc., New York, 1957), Vol. 5.

[12] L. C. Hebel and C. P. Slichter, Phys. Rev. **113**, 1504 (1959).

[13] R. V. Pound, Phys. Rev. **79**, 685 (1950).

[14] I. Waller, Z. Physik **79**, 370 (1932).

in two general classes of solids: (1) ionic solids[15–23] (notably the alkali halides) and (2) covalent solids[24] (III-V compounds).

The electric field gradients V_μ produced by a distribution of charge about a nuclear site can be expanded in powers of the relative displacements of the atoms about their equilibrium positions[25]:

$$V_\mu = A_\mu + \sum_i \mathbf{A}_{\mu i}\cdot\mathbf{r}_i + \sum_{ij}\mathbf{A}_{\mu ij}:\mathbf{r}_i\mathbf{r}_j + \cdots . \quad (6)$$

The first term is the static field gradient which does not contribute to relaxation and need not be considered further. (In the fcc structure of the rare-gas solids the static field gradient vanishes because of the cubic symmetry of the lattice.)

It can be shown[25] that the "direct process" induced by the linear term of Eq. (6) makes a negligible contribution to the nuclear relaxation time. The reason is that the first-order Hamiltonian has matrix elements only between phonon states differing by the presence of a single phonon having a frequency of ω_0 or $2\omega_0$. Since the density of phonon states is very low at the usual nuclear Larmor frequencies, the "direct" contribution is small compared to the quadratic or Raman term except at extremely low temperatures. The Raman term corresponds to absorption and emission of phonons whose frequency difference is ω_0 or $2\omega_0$. The whole frequency spectrum of the phonons is therefore available for this process.

A detailed theory of quadrupolar relaxation by the Raman process has been given by Van Kranendonk[25] for a solid with a thermal phonon spectrum described by the Debye distribution. Following the method of Van Kranendonk, one defines the functions $B_i(\mathbf{k},s)$ and $L_{sil,s'jm}$ as follows:

$$B_i(\mathbf{k},s)\equiv\delta(s,1)[\cos(\mathbf{k}\cdot\mathbf{a}_i)-1]+\delta(s,2)\sin(\mathbf{k}\cdot\mathbf{a}_i), \quad (7)$$

where $\mathbf{a}_i$ is the vector from a given atom to the nearest neighbor designated by the index i and δ is the Kronecker delta function in which s takes the values 1 and 2; and

$$L_{sil,s'jm}\equiv\{B_i(\mathbf{k},s)B_l(\mathbf{k},s)\}\{B_j(\mathbf{k}',s')B_m(\mathbf{k}',s')\}, \quad (8)$$

where the brackets indicate an average over all directions of the wave vector $\mathbf{k}$. One can then write

$$D_{sil,s'jm}(T^*)=T^*\int_0^{1/T^*}\frac{x^2e^x}{(e^x-1)^2}L_{sil,s'jm}(cT^*x)dx, \quad (9)$$

where $T^*=T/\Theta$, $c=k_ma=\sqrt{2}(3\pi^2)^{1/3}$, $x=\hbar\omega/kT$, Θ is the Debye temperature, k_m is the maximum value of the wave vector, and a is the nearest-neighbor distance. We define the quantity

$$N_{\mu ijlm}\equiv\mathbf{A}_{\mu ij}:\mathbf{A}_{\mu lm}, \quad (10)$$

where $\mathbf{A}_{\mu ij}$ is the coefficient of the second-order term $\mathbf{r}_i\mathbf{r}_j$ in Eq. (6). In terms of the foregoing definitions, the basic result of the Van Kranendonk theory[25] is that the transition probability between states m and $m+\mu$ is

$$W_{m,m+\mu}=C|Q_{\mu m}|^2T^{*2}\sum_{ss'}\sum_{ijlm}N_{\mu ijlm}D_{sil,s'jm}(T^*), \quad (11)$$

where $C=3n_0/\pi v^3d^2$, n_0 is the number of atoms per unit volume, v is the velocity of sound, and d is the mass density of the crystal. The lattice functions $D_{sil,s'jm}$ are determined by the lattice structure and the gradient functions $N_{\mu ijlm}$ depend on the distribution of charge about the nucleus.

Lattice functions. The calculation of the lattice functions $D_{sil,s'jm}$ is simplified by the fact that for the interactions considered in the rare gas solids,

$$\mathbf{A}_{\mu ijlm}=\mathbf{A}_{\mu ii}\delta_{ij}. \quad (12)$$

Thus the only lattice functions multiplied by nonvanishing $N_{\mu ijlm}$ in Eq. (11) are those of the form $D_{sil,s'il}$. Furthermore, the fcc lattice exhibits inversion symmetry and it can be shown[25] that the only nonvanishing lattice functions are those of the form $D_{sil,sil}$.

The first step in the evaluation of the lattice functions for a fcc solid is the calculation of the functions L_{silsil}. It is easily shown from (7) and (8) by elementary integration that

$$L_{1il1il}=[\tfrac{1}{2}f(k|\mathbf{a}_i+\mathbf{a}_l|)+\tfrac{1}{2}f(k|\mathbf{a}_i-\mathbf{a}_l|)-2f(ka)+1]^2, \quad (13)$$

$$L_{2il2il}=[\tfrac{1}{2}f(k|\mathbf{a}_i-\mathbf{a}_l|)-\tfrac{1}{2}f(k|\mathbf{a}_i+\mathbf{a}_l|)]^2,$$

where $f(x)=(\sin x)/x$. In a fcc solid there are only three unique functions for each value of s. These correspond to pairs of vectors to nearest-neighbor atoms, $\mathbf{a}_i$ and $\mathbf{a}_l$, such that

$$\begin{aligned}&\mathbf{a}_i\cdot\mathbf{a}_l=\pm a^2,\\ &\mathbf{a}_i\cdot\mathbf{a}_l=0,\\ &\mathbf{a}_i\cdot\mathbf{a}_l=\pm\tfrac{1}{2}a^2.\end{aligned} \quad (14)$$

If the expressions (13) are evaluated for these three

---

[15] N. Bloembergen and P. P. Sorokin, Phys. Rev. **110**, 865 (1958).
[16] O. Kraus, Bull. Am. Phys. Soc. **3**, 166 (1958).
[17] W. G. Clark, Bull. Am. Phys. Soc. **4**, 418 (1959).
[18] E. G. Wikner, W. E. Blumberg, and E. L. Hahn, Phys. Rev. **118**, 631 (1960).
[19] E. R. Andrew, K. M. Swanson, and B. R. Williams, Proc. Phys. Soc. (London) **77**, 36 (1961).
[20] W. G. Clark, thesis, Cornell University, 1961 (unpublished).
[21] P. P. Mahendroo and A. W. Nolle, Phys. Rev. **126**, 125 (1962).
[22] M. J. Weber, Phys. Rev. **130**, 1 (1963).
[23] Y. Yamagata, J. Phys. Soc. Japan **19**, 10 (1964).
[24] R. L. Mieher, Phys. Rev. **125**, 1537 (1962).
[25] J. Van Kranendonk, Physica **20**, 781 (1954).

cases, six unique $L_{sil,sil}$ are obtained:

$$\begin{aligned}
&L_1(ka)=\tfrac{1}{4}[f(2ka)-4f(ka)+3]^2 && s=1,\ \mathbf{a}_i\cdot\mathbf{a}_l=\pm a^2\\
&L_2(ka)=[f(\sqrt{2}ka)-2f(ka)+1]^2 && s=1,\ \mathbf{a}_i\cdot\mathbf{a}_l=0\\
&L_3(ka)=\tfrac{1}{4}[f(\sqrt{3}ka)-3f(ka)+2]^2 && s=1,\ \mathbf{a}_i\cdot\mathbf{a}_l=\pm\tfrac{1}{2}a^2\\
&L_4(ka)=\tfrac{1}{4}[1-f(2ka)]^2 && s=2,\ \mathbf{a}_i\cdot\mathbf{a}_l=\pm a^2\\
&L_5(ka)=0 && s=2,\ \mathbf{a}_i\cdot\mathbf{a}_l=0\\
&L_6(ka)=\tfrac{1}{4}[f(\sqrt{3}ka)-f(ka)]^2 && s=2,\ \mathbf{a}_i\cdot\mathbf{a}_l=\pm\tfrac{1}{2}a^2.
\end{aligned}\tag{15}$$

The integrals D_{silsil} may be reindexed to correspond to the six L_{silsil} functions:

$$D_n(T^*)=T^*\int_0^{1/T^*}\frac{x^2e^x}{(e^x-1)^2}L_n(cT^*x)dx. \tag{16}$$

Although the integral in Eq. (16) cannot be evaluated explicitly, the high-temperature expansion of Van Kranendonk may be employed[25]:

$$D_n(T^*)=L_{n0}-\tfrac{1}{12}L_{n2}(cT^*)^{-2}+\cdots. \tag{17}$$

The expansion coefficients are given by

$$L_{np}=c^{-1}\int_0^c x^pL_n(x)dx. \tag{18}$$

Numerical evaluation of the coefficients L_{n0} and L_{n2} then yields the following high-temperature expansions of $D_n(T^*)$ for a fcc lattice:

$$\begin{aligned}
&D_1(T^*)=1.286-0.0695T^{*-2},\\
&D_2(T^*)=0.411-0.0326T^{*-2},\\
&D_3(T^*)=0.521-0.0294T^{*-2},\\
&D_4(T^*)=0.199-0.00657T^{*-2},\\
&D_5(T^*)=0,\\
&D_6(T^*)=0.028-0.000520T^{*-2}.
\end{aligned}\tag{19}$$

In terms of the six unique lattice functions, the transition probabilities (11) may be written

$$W_{m,m+\mu}=C|Q_{\mu m}|^2T^{*2}\sum_{n=1}^{6}N_{\mu n}D_n(T^*), \tag{20}$$

in which

$$\begin{aligned}
&N_{\mu1}=N_{\mu4}=\sum_{il}{}' N_{\mu iil}, && \mathbf{a}_i\cdot\mathbf{a}_l=\pm a^2\\
&N_{\mu2}=N_{\mu5}=\sum_{il}{}' N_{\mu iil}, && \mathbf{a}_i\cdot\mathbf{a}_l=0\\
&N_{\mu3}=N_{\mu6}=\sum_{il}{}' N_{\mu iil}, && \mathbf{a}_i\cdot\mathbf{a}_l=\pm\tfrac{1}{2}a^2.
\end{aligned}\tag{21}$$

The prime on the sums in Eq. (21) indicates that the summation is to be restricted to the indicated pairs of nearest neighbors i and l.

Gradient functions. The calculation of the gradient functions $N_{\mu n}$ is carried out in three steps: (1) assumption of a suitable crystalline wave function and computation of the gradients V_μ for an arbitrary configuration of nearest-neighbor atoms; (2) expansion of the gradients to obtain $\mathbf{A}_{\mu ii}$ and hence $N_{\mu iill}$; and (3) summation of the $N\mu_{iill}$ according to Eq. (21) to obtain $N_{\mu n}$.

The contribution of exchange interactions to the electric-field gradient is obtained by assuming that the crystalline electronic wave function of the rare-gas solid is given by the overlap model of Löwdin.[26] In this model, the electron distribution about a given atom is that of a free-atom overlapping with the ground-state wave functions of its neighbors. Since exchange–van der Waals cross terms are small,[27] the contribution to the gradient from the van der Waals interactions may be considered separately and added to the exchange contribution.

If the position of the ith neighbor is denoted by the direction cosines α_i, β_i, γ_i the gradients (2) may be written

$$\begin{aligned}
V_0&=\textstyle\sum_i\lambda_i(\gamma_i^2-\frac{1}{3}),\\
V_{\pm1}&=\textstyle\sum_i\lambda_i\gamma_i(\alpha_i\pm i\beta_i),\\
V_{\pm2}&=\tfrac{1}{2}\textstyle\sum_i\lambda_i(\alpha_i\pm i\beta_i)^2.
\end{aligned}\tag{22}$$

The contribution of exchange effects to the quadrupole interaction is then given by the theory of Kondo and Yamashita[28]:

$$\lambda_i^{\rm ex}=-(12e/5)\langle r^{-3}\rangle_{np}(S_{\sigma s}^2+S_{\sigma\sigma}^2-S_{\pi\pi}^2), \tag{23}$$

where

$$S_{\mu\nu}=\int\phi_\mu^*(r)\phi_\nu(r)dr-\delta_{\mu\nu}, \tag{24}$$

and the average $\langle r^{-3}\rangle_{np}$ is taken over the outer p states with $n=2,3,4,5$ for Ne, Ar, Kr, Xe, respectively. The σ and π orbitals in Eq. (23) are p states directed parallel and perpendicular, respectively, to the vector from the atom of interest to the ith neighbor. Adrian[27] has computed the contribution to the quadrupole coupling of the van der Waals interaction and has found

$$\lambda_i^{VdW}=(9e/20)\alpha_p^2R^{-6}\langle r^{-3}\rangle_{np}, \tag{25}$$

where α_p is the atomic polarizability of the rare gas. Thus,

$$\lambda_i=(3e/5)\langle r^{-3}\rangle_{np}[\tfrac{3}{4}\alpha_p^2R^{-6}-4(S_{\sigma s}^2+S_{\sigma\sigma}^2-S_{\pi\pi}^2)]. \tag{26}$$

The gradients (22) can be expanded in a straightforward manner to obtain the functions $N_{\mu iill}$. When these functions are summed over the twelve nearest neighbors in the face-centered cubic lattice a rather

[26] P. O. Löwdin, Ark. Mat. Astron. Fysik **35A**, No. 9 (1948).
[27] F. J. Adrian, Phys. Rev. **138**, A403 (1965).
[28] J. Kondo and J. Yamashita, J. Phys. Chem. Solids **10**, 245 (1959).

lengthy calculation yields the six gradient functions:

$$N_{11}=N_{14}=4a^{-4}[(35u^2+v^2+6\lambda^2+10uv+16\lambda u+2\lambda v)-\alpha^2(19u^2+v^2+10uv+2\lambda v)],$$
$$N_{12}=N_{15}=4a^{-4}[(-11u^2+6\lambda^2-2uv+16\lambda u+2\lambda v)+\alpha^2(57u^2+6uv-2\lambda v)],$$
$$N_{13}=N_{16}=8a^{-4}[(20u^2+12\lambda^2+4uv+32\lambda u+4\lambda v)-\alpha^2(19u^2+\tfrac{1}{4}v^2+6uv+4\lambda v)], \quad (27)$$
$$N_{21}=N_{24}=a^{-4}[(121u^2+3v^2+24\lambda^2+30uv+64\lambda u+6\lambda v)+\alpha^2(19u^2+v^2+10uv+2\lambda v)],$$
$$N_{22}=N_{25}=a^{-4}[(13u^2+24\lambda^2-2uv+64\lambda u+6\lambda v)+\alpha^2(-57u^2-6uv+2\lambda v)],$$
$$N_{23}=N_{26}=2a^{-4}[(61u^2-\tfrac{1}{4}v^2+48\lambda^2+10uv+128\lambda u+12\lambda v)+\alpha^2(19u^2+\tfrac{1}{4}v^2+6uv+4\lambda v)],$$

where

$$u\equiv\tfrac{1}{2}a\lambda'-\lambda, \quad v\equiv 4\lambda-\tfrac{5}{2}a\lambda'+\tfrac{1}{2}a^2\lambda'' \quad (28)$$

and the prime represents differentiation with respect to R. The dependence of the transition probabilities on the orientation of the crystal is contained in the terms proportional to

$$\alpha^2=\alpha_H^2\beta_H^2+\alpha_H^2\gamma_H^2+\beta_H^2\gamma_H^2, \quad (29)$$

where α_H, β_H, γ_H are the direction cosines of the magnetic field relative to the crystalline axes.

Evaluation for solid xenon. The gradient functions for solid xenon were evaluated numerically from Eq. (26) using the atomic parameters and overlap integrals employed by Adrian for calculating T_1 for Xe^{131} in the gas. Substitution of these functions and the high-temperature expansions of the lattice functions into Eq. (20) yields the following expressions for the transition probabilities for Xe^{131} in solid xenon:

$$W_1=(2.24\times10^{-3})T^{*2}[(67.3-77.1\alpha^2)-T^{*-2}(3.56-4.16\alpha^2)]$$
$$W_2=(0.56\times10^{-3})T^{*2}[(196+77.1\alpha^2)-T^{*-2}(10.1+4.16\alpha^2)]. \quad (30)$$

In evaluating the constant C, the velocity of sound was estimated by assuming the Debye temperature to be 55°K[29] and using the values of the density and lattice constant at 100°K. Since $T_2\ll T_1$ at 100°K, Eq. (5) may be employed to obtain

$$T_1=1.3 \text{ sec}.$$

The angular dependence exhibited by the transition probabilities vanishes when the probabilities are added in Eq. (5). Thus, when a spin temperature can be assumed, the theory predicts an isotropic relaxation time for a fcc single crystal. The same result has been found previously for other crystals exhibiting cubic symmetry.[24]

[29] A. C. Hollis Hallet, in G. A. Cook, *Argon, Helium and the Rare Gases* (Interscience Publishers, Inc., New York, 1961), Vol. 1, Chap. IX.

At temperatures well above the Debye temperature, the terms proportional to $(T^*)^{-2}$ in Eq. (30) are small and the theory predicts that the transition probabilities vary as T^{*2}. To obtain the approximate temperature dependence in the region where $T^*<1$, one can follow the procedure used by Van Kranendonk[25] for the NaCl lattice and write

$$\sum_{n=1}^{6} N_{\mu n}D_n(T^*)=E_\mu(\infty)E(T^*). \quad (31)$$

The function $E(T^*)$ has been evaluated numerically by Van Kranendonk. Since $E(T^*)$ is unity when $T^*\gg1$, the $E_\mu(\infty)$ can be obtained from Eq. (27) and the first terms of Eq. (19). The temperature dependence of T_1 should thus be given by

$$1/T_1\propto T^{*2}E(T^*). \quad (32)$$

Application of the theory of quadrupole relaxation via the Raman process to the case of Xe^{131} in solid xenon yields two principal results which may be compared with experiment. Comparison of the predicted magnitude of T_1 with experiment provides a test of the overlap–van der Waals model used to calculate the strength of the time-dependent electric-field gradients. The temperature dependence of the data may be compared with Eq. (32) to determine whether the Raman process is, in fact, responsible for relaxation and to obtain information about the Debye temperature of solid xenon.

2. *Quadrupole Relaxation via Random Atomic Motions*

In rare-gas solids at temperatures near the melting points and in the liquids, random time-dependent electric-field gradients produced by self-diffusion and diffusion of crystalline defects provide a potential relaxation mechanism for quadrupolar nuclei.[11] By applying the usual methods of time-dependent perturbation theory to the case of a randomly varying quadrupole interaction[30] it can be seen easily that the transition probabilities are

$$W_\mu=\frac{1}{12}\left(\frac{eQ}{\hbar}\right)^2 J^\mu(\mu\omega_0). \quad (33)$$

The spectral functions $J^\mu(\omega_{mn})$ are the Fourier transforms of the time-correlation functions of the random electric-field gradients,

$$g_\mu(t)=\langle V_{-\mu}(t)V_\mu(t+\tau)\rangle. \quad (34)$$

The transition probabilities are maximum when the correlation time τ is approximately $1/\omega_0$ or $1/2\omega_0$ for transitions of $\Delta m=\pm1$ or $\Delta m=\pm2$, respectively.

Detailed calculation of the correlation functions for gradients produced by diffusing defects (vacancies and

[30] A. Abragam, *The Principles of Nuclear Magnetism* (Clarendon Press, Oxford, England, 1961).

impurities) in a rare-gas solid is difficult because of limited knowledge of the spatial dependence of the gradients produced by such defects. In the liquid, on the other hand, one might assume that the gradients arise from exchange and van der Waals interactions between neighboring xenon atoms. In this case, however, the calculation of correlation functions is hindered by the lack of an adequate model for the microscopic atomic motions.

If one makes the assumption of an exponential correlation function

$$g_\mu(t)=\langle V_{-\mu}(0)V_\mu(0)\rangle e^{-t/\tau}, \tag{35}$$

the spectral functions can be obtained immediately:

$$J^1(\omega_0)=\langle V_{-1}(0)V_1(0)\rangle\frac{2\tau}{1+\omega_0^2\tau^2},$$
$$J^2(2\omega_0)=\langle V_{-2}(0)V_2(0)\rangle\frac{2\tau}{1+4\omega_0^2\tau^2}. \tag{36}$$

In this simple case, the quadrupolar spectral functions are similar to those for dipolar relaxation due to random atomic motion. For translational diffusion one would expect the correlation time τ to be proportional and, if $\omega_0\tau\ll 1$, the relaxation time to be inversely proportional to the coefficient of self-diffusion.[31]

B. Experimental Results and Interpretation

1. *Spin-Lattice Relaxation in Solid Xenon*

Spin-lattice relaxation was observed in solid xenon from 9°K to the melting point (161°K). Throughout this temperature range the nuclear magnetization recovered to equilibrium with simple exponential time dependence and a single T_1 could be assigned. The observation of single exponential recovery at the higher temperatures where Eq. (5) is not valid ($T_1\approx T_2$) can be understood in terms of the probabilities (30) evaluated for a polycrystalline sample.[32] If α^2 is averaged over all possible orientations of the crystal axes with respect to the magnetic field, it turns out that

$$W_1=W_2=W.$$

On the basis of Eq. (3) therefore, one would expect exponential recovery to equilibrium with a single time constant $1/2W$.

The observed values of T_1 are plotted in Fig. 1. The relaxation time increases monotonically with decreasing temperature from a value of about 200 msec at the melting point to 390 sec at 9°K. These values are orders of magnitude shorter than the corresponding Xe^{129} relaxation times indicating that quadrupole interactions are responsible for relaxation. Data were not taken at temperatures below 9°K because of the difficulty of maintaining stable sample temperatures for periods of several T_1's. At 4.2°K, paramagnetic impurities were probably responsible for the observed spin-lattice relaxation since at this temperature, the Xe^{129} relaxation time was shorter than the $Xe^{131}T_1$. At all other temperatures measured the $Xe^{131}T_1$ was shorter than that for Xe^{129}. For the purest samples used, the Xe^{131} relaxation time at 4.2°K was greater than 1 h.

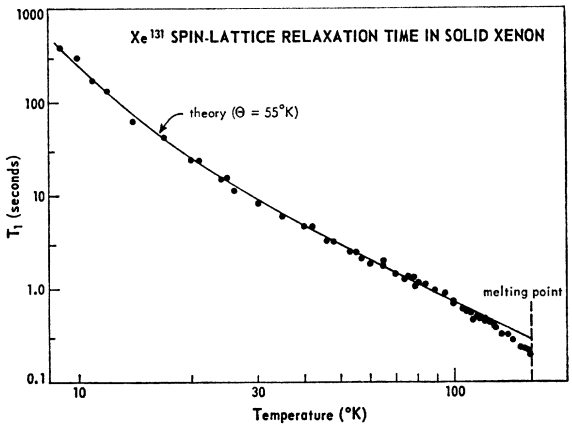

FIG. 1. Spin-lattice relaxation times of Xe^{131} in solid xenon. The solid line represents the temperature dependence of Eq. (32) normalized to the data at 77°K.

The solid line in Fig. 1 represents the temperature dependence predicted by the theory for quadrupole relaxation via the two-phonon Raman process. The theoretical curve has been normalized to the data at 77°K and the Debye temperature of solid xenon has been taken to be 55°K. The implicit temperature dependence resulting from variation of the strength of the quadrupole interaction with thermal expansion of the lattice has been neglected. It was found by numerical evaluation of the various parameters that the temperature dependence of Eq. (20) is contained in Eq. (30) to within roughly the accuracy of the data.

It can be seen from Fig. 1 that the temperature dependence of the data agrees well with the prediction except in the vicinity of the melting point. At temperatures above the Debye temperature $1/T_1$ varies approximately as T^2 while at low temperatures, the departure from T^2 dependence is predicted very well by the Van Kranendonk function. The normalized low-temperature data have been divided by T^{*2} and plotted in Fig. 2 for direct comparison with the Van Kranendonk function $E(T^*)$. In spite of the increased scatter of the data, it is evident that the Van Kranendonk function accurately describes the temperature dependence of T_1 down to $T^*\approx 0.16$.

Above 100°K, the data vary somewhat more rapidly with temperature than the theory predicts for a Debye temperature of 55°K. The discrepancy can be seen in Fig. 3 where the solid line corresponds to $1/T_1\propto T^2$ and the solid points are the "clean" sample T_1 data. This

[31] N. Bloembergen, E. M. Purcell, and R. V. Pound, Phys. Rev. 73, 679 (1948).

[32] The spin phase-memory times will be discussed in a subsequent paper.

failure of Eq. (32) to predict the correct temperature dependence may be a consequence of the failure of the Debye approximation to represent the true phonon spectrum of the solid. The inherent error of the Debye spectrum is often described by a temperature-dependent Debye temperature. Packard and Swenson[33] have obtained the temperature dependence of Θ at zero pressure from experimental values of the heat capacity of solid xenon. If these results are used to determine T^*, the predicted temperature dependence (indicated by the broken line of Fig. 3) is in excellent agreement with the data. This agreement is particularly interesting in that the Θ obtained from heat-capacity measurements results from a different average over the phonon spectrum than that which occurs in the theory of quadrupole relaxation.

The observed magnitude of T_1 at 100°K is

$$T_1 = 0.70 \pm 0.05 \text{ sec}, \qquad \text{(experiment)}$$

which is to be compared with the theoretical value obtained in the previous section by considering the effects of exchange and Van der Waals interactions,

$$T_1 = 1.3 \text{ sec}. \qquad \text{(theory)}$$

In view of the approximations of the model, agreement between theory and experiment is quite good.

The fact that the quadrupole-phonon interaction apparently accounts for spin-lattice relaxation in "clean" solid xenon at temperatures near the melting point indicates that the quadrupolar interaction with time-dependent electric-field gradients produced by diffusing vacancies is not an effective relaxation process.

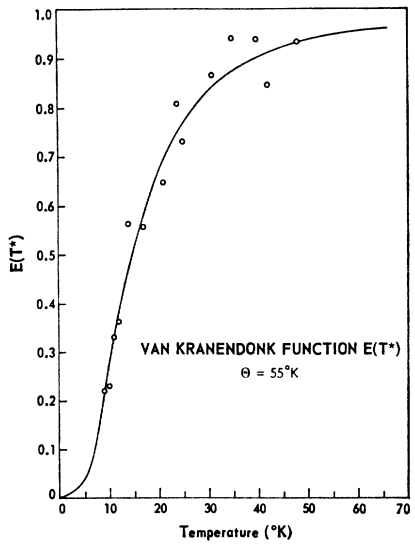

FIG. 2. The Van Kranendonk function $E(T^*)$. The data are normalized to Eq. (32) at 77°K and divided by T^{*2} to obtain $E(T^*)$.

[33] J. R. Packard and C. A. Swenson, J. Phys. Chem. Solids **24**, 1405 (1963).

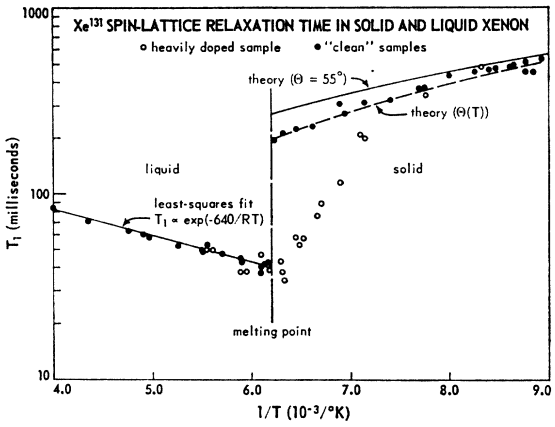

FIG. 3. Spin-lattice relaxation times of Xe^{131} in liquid and solid xenon. The solid line through the liquid data is a least-squares fit to an exponential temperature dependence. The solid line on the right-hand portion of the graph represents Eq. (32) with $\Theta = 55$°K normalized to the data at 77°K. The broken line represents Eq. (32) normalized to 77°K with $\Theta(T)$ as given by Packard and Swenson in Ref. 33.

On the other hand, diffusing impurities can be an important mechanism. Data taken in samples having an impurity (air) concentration of 10^{-2} to 10^{-3} demonstrate a striking decrease in T_1 at temperatures near the melting point. These data are represented by the open circles in Fig. 3. Since the $Xe^{131} T_1$ values were still at least an order of magnitude shorter than the Xe^{129} relaxation times in the same samples, it can be concluded that dipolar interactions with paramagnetic oxygen are not effective and that the observed effect must arise from quadrupole relaxation via diffusing impurities. Unfortunately, the impurity concentration was not known accurately enough to permit a meaningful estimate of the magnitude of the gradients produced by the impurity molecules.

2. *Spin-Lattice Relaxation in Liquid Xenon*

Spin-lattice relaxation times for Xe^{131} in liquid xenon were measured from the melting point to 250°K. A pressure of 30 atm was applied to the sample to extend the liquid range to the higher temperature. No pressure-dependent effects on the nuclear-relaxation process were observed. Recovery of the magnetization appeared to be governed by a single exponential so that unique T_1 values could be determined. These data are plotted against $1/T$ in Fig. 3 and exhibit the following principal features: (1) T_1 values in the liquid appear to be independent of impurity content (including helium from the pressure medium); (2) the value of T_1 decreases by about a factor of 5 when the sample melts; (3) the temperature dependence of T_1 appears to be exponential with the form

$$T_1 \propto \exp(-E_A/RT). \qquad (37)$$

E_A is an "activation energy" for the thermal motion producing relaxation. A least-squares fit of the data

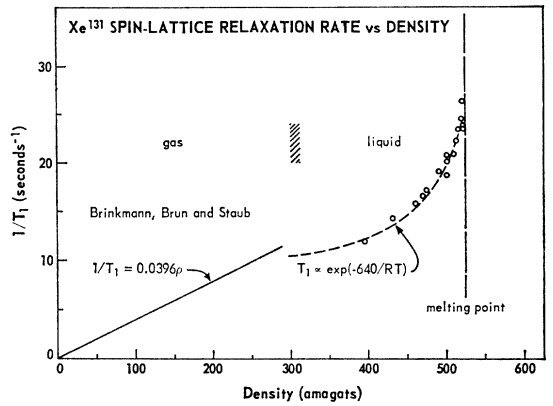

FIG. 4. Spin-lattice relaxation rate $1/T_1$ of Xe^{131} in liquid xenon. The broken line represents a least-squares fit to an exponential temperature dependence. The solid line represents the data of Brinkmann, Brun, and Staub (Ref. 34).

to the temperature dependence (37) yields

$$E_A = 640 \pm 30 \quad \text{cal/mole}.$$

The relaxation rate $1/T_1$ is plotted as a function of density in Fig. 4 using the liquid density data tabulated by Hollis Hallet.[29] The broken line represents the least-squares fit to exponential temperature dependence Also shown in Fig. 4 are the data of Brinkman, Brun, and Staub[34] for Xe^{131} relaxation in gaseous xenon at 25°C. These data show that in the gas, the relaxation rate is proportional to the density. If the present Xe^{131} data are extrapolated to lower values of the density it appears that the results are in good agreement with the high-density-gas data.

The fact that the data appear to exhibit exponential temperature dependence would suggest that spin-lattice relaxation is caused by atomic diffusion. On the basis of a simple diffusion model[31] of the liquid, one would expect correlation functions of the form (36) in which the correlation time τ is proportional to the coefficient of self-diffusion. If this model is assumed, then it can be determined from the diffusion data of Yen and Norberg[3] that the condition of extreme narrowing, $\omega_0\tau \ll 1$, holds for Xe^{131} in liquid xenon. This conclusion is supported by the fact that T_1 is equal to T_2. In the extreme narrowing limit, the transition probabilities are, from Eq. (36),

$$W_1 = \tfrac{1}{6}(eQ/\hbar)^2 \langle V_{-1}(0) V_1(0) \rangle \tau,$$
$$W_2 = \tfrac{1}{6}(eQ/\hbar)^2 \langle V_{-2}(0) V_2(0) \rangle \tau. \qquad (38)$$

For relaxation behavior described by a single exponential, the simple diffusion model then predicts

$$T_1 \propto 1/\tau \propto D_0 \exp(-E_D/RT), \qquad (39)$$

where D_0 is the diffusion constant and E_D is the activation energy for self-diffusion. The activation energy has been measured by Yen and Norberg using spin-echo techniques in an applied magnetic-field gradient, and by Naghizadeh and Rice[35] by radioactive tracer techniques. These measurements yield

$$E_D = 1400 \pm 150 \text{ cal/mole} \quad \text{(Yen and Norberg)},$$
$$E_D = 1210 \text{ cal/mole} \quad \text{(Naghizadeh and Rice)}.$$

The "activation energy" inferred from quadrupole relaxation of Xe^{131} is approximately half the average of these two results. The discrepancy is well outside experimental error and clearly indicates that Xe^{131} relaxation in the liquid cannot be adequately explained by a simple diffusion model.

IV. CHEMICAL SHIFTS

Investigations of the nuclear-magnetic resonance of Xe^{129} have disclosed the existence of density-dependent shifts of the resonance frequency in all three phases of xenon. Streever and Carr[1] and Hunt and Carr[2] have shown by pulsed NMR measurements that the local field in gaseous and liquid xenon increases linearly with increasing density at constant applied field. Later work by Yen and Norberg[3] on Xe^{129} showed that the local field increases linearly with density even more rapidly in solid xenon. These measurements indicate that as the density of xenon atoms increases, the atomic electrons become less effective in shielding the nucleus from the external field. The data show, for example, that the diamagnetic shielding parameter of the liquid is about 3% smaller than that of an isolated atom.

It was the purpose of the present work to extend resonance shift measurements to Xe^{131} for two principal reasons. First, the short quadrupolar relaxation times of Xe^{131} eliminated the need to introduce paramagnetic impurities to obtain workable relaxation times. The possibility of erroneous results due to the presence of such impurities was therefore greatly reduced. Second, if the shifts are produced by density-dependent modification of the diamagnetic shielding, the observed changes of the local field should be the same for either isotope. Xe^{131} measurements thus provide a means for verifying that the shift is, in fact, an electronic phenomenon or "chemical" shift.

Xe^{131} resonance shifts were measured in solid and liquid xenon from 4.2 to 250°K. The measurements yielded shifts of the external resonant field relative to the resonant field at a reference temperature chosen arbitrarily to be 130°K. The data are plotted as a function of density in Fig. 5 using the molar volume data of Packard and Swenson[33] for the solid and the liquid-density data tabulated by Hollis Hallet[29] for conversion from temperature to density. The broken and solid lines in Fig. 5 represent least-squares fits to linear density dependences for the liquid and solid,

[34] D. Brinkmann, E. Brun, and H. H. Staub, Helv. Phys. Acta 35, 431 (1962).

[35] J. Naghizadeh and S. A. Rice, J. Chem. Phys. 36, 2710 (1962).

respectively. The slopes are

$$\text{liquid:}\quad -\frac{1}{H_0}\frac{\partial(\Delta H)}{\partial\rho}=(5.1\pm0.5)\times10^{-7}\quad(\text{amagat})^{-1}$$

$$\text{solid:}\quad -\frac{1}{H_0}\frac{\partial(\Delta H)}{\partial\rho}=(18.2\pm1.1)\times10^{-7}\quad(\text{amagat})^{-1}.$$

The dotted line in Fig. 5 represents the Xe^{129} resonance shift in solid xenon measured by Yen and Norberg:

$$-\frac{1}{H_0}\frac{\partial(\Delta H)}{\partial\rho}=20.4\times10^{-7}\quad(\text{amagat})^{-1}.$$

It is clear that the density dependence of the shielding is essentially the same for both isotopes.

A striking feature of these data is the change of the density dependence of the shift at the melting point. The ratio of solid slope to liquid slope is 3.6. This ratio is in marked contrast to recent results of Brinkmann and Carr[4,36] who have found nearly the same average density dependence in the solid as in the liquid:

$$\text{liquid:}\quad -\frac{1}{H_0}\frac{\partial(\Delta H)}{\partial\rho}=5.66\times10^{-7}\quad(\text{amagat})^{-1}$$

$$\text{solid:}\quad -\frac{1}{H_0}\frac{\partial(\Delta H)}{\partial\rho}=(5.10\times10^{-6})-(7.42\times10^{-9})\rho\quad(\text{amagat})^{-1}.$$

The shift at the melting point found by Brinkmann and Carr at 7100 G is (when adjusted to our field)

$$(\Delta H)_{mp}=0.42\pm0.04\text{ G}\quad\text{(Brinkmann and Carr)}$$

and is in good agreement with our observed Xe^{131} melting point shift:

$$(\Delta H)_{mp}=0.37\pm0.10\text{ G}.$$

The source of the discrepancy between the present solid data and those of Yen and Norberg on the one hand, and the results of Brinkmann and Carr on the other, remains unknown. The possibility of systematic calibration errors seems remote since several means of checking the calibration were available. The agreement of the Xe^{131} liquid data with those of Brinkmann and Carr supports this conclusion. Furthermore, since three fixed points for thermometry calibrations were available in the solid range (He boiling point, N_2 boiling point, Xe boiling point), large errors in temperature measurement seem quite unlikely. The remaining possible source for the discrepancy is then the condition of the solid xenon samples themselves.

Xe^{131} shift measurements were made with both "clean" samples and air-doped samples showing large impurity relaxation effects. No dependence of the shift on impurity content was observed. Similarly, Brinkmann and Carr have searched for impurity effects in their measurements and have found none.

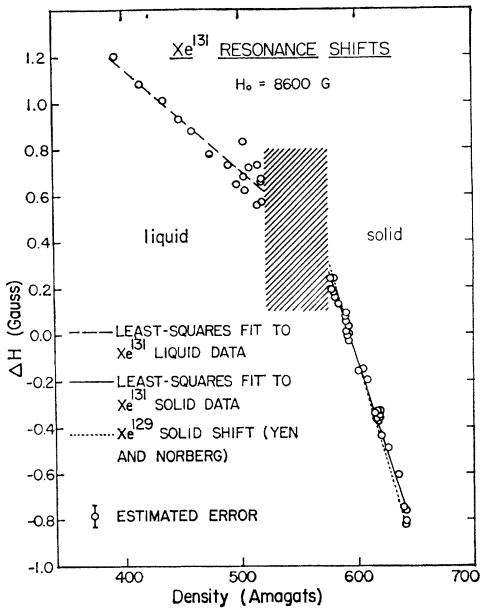

FIG. 5. Relative Xe^{131} shifts in liquid and solid xenon. ΔH is the change in external resonant field relative to the resonant field at 130°K.

The Xe^{131} measurements were made in a nylon sample container. Since the volume of the chamber decreased by only about 2% when cooled from 160 to 4.2°K while the xenon sample contracted about 10%, there should have been no compression of the samples at low temperatures. On the other hand, the possibility remains that additional xenon could condense into the chamber at low temperatures so that as the sample warmed up, the greater expansion coefficient of the xenon would produce compression of the samples. To prevent this, the experiments were performed with the sample chamber only about $\frac{3}{4}$ full to provide volume for thermal expansion. The absence of hysteresis in the shifts as the sample was cooled below the reference temperature and then rewarmed indicates that effects due to compression of the sample during warmup were small.

An approximate value of the absolute local field shift relative to the isolated atom was obtained by fitting the Xe^{131} liquid data to the Xe^{129} liquid absolute shift data of Hunt and Carr. The result is shown in Fig. 6; the solid line represents the least-squares fit of Hunt and Carr. The data indicate that the local field in the solid at 0°K is increased relative to the isolated atom (i.e., gas at zero density) at 8600 G by

$$(\Delta H)_0=3.3\pm0.1\text{ G}.$$

Adrian[37] has applied the general theory of chemical shifts to the case of xenon atoms undergoing binary

[36] D. Brinkmann and H. Y. Carr (private communication).

[37] F. J. Adrian, Phys. Rev. 136, A980 (1964).

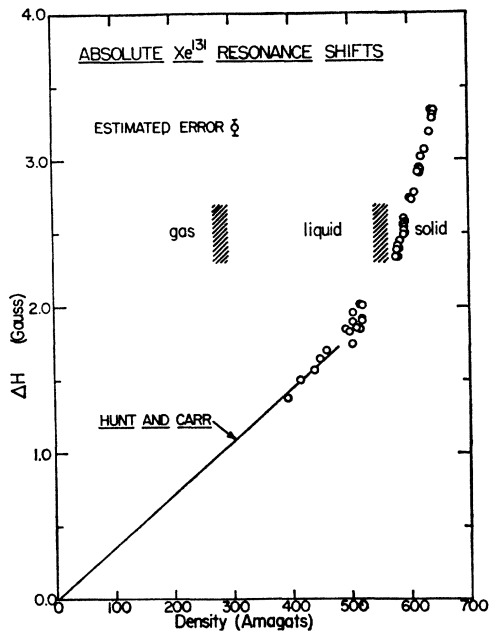

FIG. 6. Absolute Xe^{131} local field shifts in liquid and solid xenon. The liquid data have been normalized to the solid line representing the data of Hunt and Carr (Ref. 2).

collisions in the gas. He has considered the effects of both exchange and van der Waals interactions in deforming the electron clouds during collisions and found that the exchange interaction makes the dominant contribution. If Adrian's expression for the shift produced by a single neighbor is summed over the twelve nearest neighbors in the fcc lattice, the shift of the local field in the solid (relative to the isolated atom) is found to be

$$\Delta H=\frac{128\mu_\beta^2}{\langle\Delta E\rangle}\langle r^{-3}\rangle_{5p}(S_{\sigma\sigma}^2+S_{\pi\pi}^2)H_0. \qquad (40)$$

In Eq. (40), μ_β is the Bohr magneton, $\langle\Delta E\rangle$ is the average energy of the atomic excited states, and the overlap integrals are defined by Eq. (24). If the numerical values of $\langle\Delta E\rangle$, $\langle r^{-3}\rangle_{5p}$, and $(S_{\sigma\sigma}^2+S_{\pi\pi}^2)$ used by Adrian are employed, the absolute shift at 0°K in a field of 8600 G predicted by Eq. (40) is

$$(\Delta H)_0=2.0 \text{ G}.$$

This result is in fair agreement with the experimental value, $(\Delta H)_0=3.3\pm0.1$ G. The ratio $(\Delta H)_0$(experiment)/$(\Delta H)_0$(theory) for the solid (about 1.7) is to be compared with the corresponding ratio (about 1.5) comparing Adrian's theory with the gas data of Hunt and Carr. This correspondence suggests that the errors in the theory result from certain approximations which are used in both calculations, i.e., the "average energy approximation."

A complete theory of the shift in the solid must include the effects of the lattice vibrations. Adrian[38] has recently computed the temperature dependence of the solid shift, taking into account both thermal expansion and lattice vibrations, and obtains a value for $\delta(\Delta H)/\delta T$ which is in somewhat better agreement with the present Xe^{131} results than with the data of Brinkmann and Carr. However, the approximations of the theory are such that this agreement cannot be regarded as convincing evidence in favor of the one set of experimental results over the other.

V. CONCLUSIONS

It may be concluded from the observed temperature dependence of the $Xe^{131}T_1$ that spin-lattice relaxation in "clean" solid xenon samples arises from the two-phonon Raman process. Furthermore, the agreement of experiment and theory for the magnitude of T_1 at 100°K is good evidence for the general validity of the Van Kranendonk theory and indicates that the overlap model with van der Waals interactions provides a realistic description of the electronic configuration in solid xenon. The latter conclusion is supported by the fair success of the same model when applied to the calculation of the absolute chemical shift at 0°K. In the case of the chemical shift, however, the approximations used in the theory and the conflicting experimental results with regard to the temperature dependence make it difficult to draw more definite conclusions at this time.

The observation of quadrupole relaxation indicates that large time-dependent electric field gradients are experienced by nuclei in liquid xenon. These gradients presumably result from the same deformations of the atomic charge distributions that lead to the chemical shifts in the liquid. The failure of the simple diffusion model to account for the temperature dependence of T_1 suggests that more sophisticated models of the structure and thermal motions of the liquid are required. There clearly exists a need for detailed calculations of quadrupole relaxation and chemical shifts in monatomic liquids using various models of the liquid state.

ACKNOWLEDGMENTS

The authors wish to express their appreciation to H. Y. Carr and D. Brinkmann for their communications regarding the progress of the shift measurements at Rutgers University. We are also indebted to F. J. Adrian for supplying the results of his calculations prior to publication. We wish to thank K. Luszczynski for a number of helpful suggestions concerning various phases of our experiments. W. G. Clark kindly read the manuscript and offered several valuable comments.

[38] F. J. Adrian (private communication).